European Journal of Medicinal Chemistry 188 (2020) 112030

Contents lists available at ScienceDirect

European Journal of Medicinal Chemistry

journal homepage: http://www.elsevier.com/locate/ejmech

Research paper

Synthesis and biological assessment of a ruthenium(II) cyclopentadienyl complex in breast cancer cells and on the development of zebrafish embryos

Golara Golbaghi, Irène Pitard, Matthieu Lucas, Mohammad Mehdi Haghdoost, Yossef López de los Santos, Nicolas Doucet, Shunmoogum A. Patten, J. Thomas Sanderson, Annie Castonguay*

Organometallic Chemistry Laboratory for the Design of Catalysts and Therapeutics, and Endocrine Toxicology Laboratory, INRS-Centre Armand-Frappier Santé Biotechnologie, Université du Québec, Laval, Canada

ARTICLE INFO

Article history:
Received 31 October 2019
Received in revised form
17 December 2019
Accepted 30 December 2019
Available online 3 January 2020

Keywords:
Ruthenium complex
Breast cancer therapy
Estrogen receptor positive breast cancer
Triple negative breast cancer
Aromatase inhibitor
Zebrafish

ABSTRACT

Ruthenium-based complexes currently attract great attention as they hold promise to replace platinum-based drugs as a first line cancer treatment. Whereas ruthenium arene complexes are some of the most studied species for their potential anticancer properties, other types of ruthenium complexes have been overlooked for this purpose. Here, we report the synthesis and characterization of Ru(II) cyclopentadienyl (Cp), Ru(II) cyclooctadienyl (COD) and Ru(III) complexes bearing anastrozole or letrozole ligands, third-generation aromatase inhibitors currently used for the treatment of estrogen receptor positive (ER +) breast cancer. Among these complexes, Ru(II)Cp **2** was the only one that displayed a high stability in DMSO and in cell culture media and consequently, the only complex for which the *in vitro* and *in vivo* biological activities were investigated. Unlike anastrozole alone, complex **2** was considerably cytotoxic *in vitro* (IC_{50} values < 1 μM) in human ER + breast cancer (T47D and MCF7), triple negative breast cancer (TNBC) (MBA-MB-231), and in adrenocortical carcinoma (H295R) cells. Theoretical (docking simulation) and experimental (aromatase catalytic activity) studies suggested that an interaction between **2** and the aromatase enzyme was not likely to occur and that the bulkiness of the PPh_3 ligands could be an important factor preventing the complex to reach the active site of the enzyme. Exposure of zebrafish embryos to complex **2** at concentrations around its *in vitro* cytotoxicity IC_{50} value (0.1−1 μM) did not lead to noticeable signs of toxicity over 96 h, making it a suitable candidate for further *in vivo* investigations. This study confirms the potential of Ru(II)Cp complexes for breast cancer therapy, more specifically against TNBCs that are usually not responsive to currently used chemotherapeutic agents.

1. Introduction

Metal complexes are a useful class of molecules with a broad spectrum of therapeutic applications. Despite the considerable success of platinum-based anticancer agents, which are administered to nearly 50% of patients undergoing chemotherapy, factors such as severe side effects and emergence of cancer cell resistance limit their clinical applications [1–4]. In the past years, ruthenium compounds have attracted increasing attention and are often considered potential alternatives to platinum drugs given their selective bioactivity and their ability to overcome platinum-mediated cancer cell resistance. They are known for their cytotoxicity and/or their antimetastatic properties through distinct mechanisms of action, notably DNA or protein binding, reactive oxygen species (ROS) generation and cancer cell mobility inhibition [1,5–7]. Importantly, several ruthenium complexes have entered and/or are currently in various stages of clinical trials [8–15]. Of particular interest is the design of organoruthenium complexes bearing carefully selected biologically active ligands such as enzyme inhibitors involved in the treatment of cancer, allowing the development of efficient drug/prodrug candidates that can display multiple modes of action. This strategy can potentially circumvent

* Corresponding author.
E-mail address: annie.castonguay@inrs.ca (A. Castonguay).

https://doi.org/10.1016/j.ejmech.2019.112030
0223-5234/

emerging drug resistance mechanisms, a common cause of mortality in cancer patients [16–19]. For instance, we reasoned that third-generation aromatase inhibitors such as the nonsteroidal triazole derivatives anastrozole (Arimidex®) and letrozole (Femara®) could be suitable candidates for this purpose, as they are widely used to treat estrogen receptor positive (ER +) breast cancer in postmenopausal women, and have the ability to coordinate ruthenium [20]. ER + breast cancer cells proliferate under the influence of elevated estrogen levels, but are deprived of this hormone by aromatase inhibitors, which act by preventing the aromatase-catalyzed production of estrogens from androgens [21]. Despite the success of third generation aromatase inhibitors for the treatment of breast cancer, in approximately one third of patients diagnosed with metastatic ER + breast cancer, therapies involving these drugs lead to the mutation of the ER gene, resulting in a treatment-resistant cancer that is often incurable [22,23]. Furthermore, estrogen deprivation was previously reported to sensitize ER + breast cancer cells to cytotoxic agents [24,25].

We recently reported the biological activity of a series of half-sandwich ruthenium (II) arene complexes with anastrozole ligands [26]. This previous study followed a preliminary investigation by Maysinger et al. on the cytotoxicity of a series of ruthenium (II) arene complexes bearing letrozole ligands [16]. To get more insights into the potential effectiveness of ruthenium-anastrozole complexes in cancer therapy, we were interested in exploring the physical and biological properties of structurally and electronically diverse types of ruthenium complexes. Although half-sandwich ruthenium (II) arene complexes have been extensively investigated for their ability to induce cancer cell toxicity and, in some cases, with high selectivity toward cancer cells [27–29], there are far fewer studies of the anticancer potential of ruthenium (II) complexes based on cyclooctadiene (COD) or cyclopentadiene (Cp) ligands [30–41]. For instance, Sheldrick et al. reported a cationic Ru(II)COD complex with considerable cytotoxicity in Jurkat leukemia cells, for which the mode of action is believed to be associated with the generation of reactive oxygen species (ROS) [41]. Another report from Omondi revealed that a series of Ru(II)COD complexes with bidentate N,N-donor ligands had a high affinity with human serum albumin (HSA). However, the cytotoxicity of these complexes was not investigated [33]. Promising anticancer activities were also reported for some Ru(II)Cp complexes [34,42–47]. For instance, it was shown by Severin et al. that replacing the arene ligand in the structure of a RAPTA-type complex, [(η^6-arene)$RuCl_2$(PTA)] (PTA = 1,3,5-triaza-7-phosphaadamantane), with a bulky cyclopentadienyl electron-donating ligand led to compounds with enhanced cytotoxicities [43,44]. This effect is believed to be associated with the improved ability of the complexes to cross cancer cell membranes [43]. Notably, Garcia et al. reported a new family of Ru(II)Cp complexes with N,O- and N,N′-heteroaromatic bidentate ligands that revealed an exceptional activity with IC_{50} values in the nanomolar range against the MDA-MB-231 breast cancer cell line [45,47]. They also investigated the *in vivo* antitumor activity of a Ru(II)Cp (TM90, [Ru(η^5-C_5H_5)(PPh_3)(bopy)] [CF_3SO_3] (bopy = 2-benzoylpyridine) on nude female mice bearing TNBC orthotopic tumors. Importantly, the study revealed the ability of the complex to suppress tumor growth and to inhibit the development of metastases, to increase the lifetime of mice after surgical removal of the tumor (compared to untreated mice) and to not negatively affect their behavior [42]. Fernandes et al. synthesized and characterized a series of Ru(II)Cp complexes bearing carbohydrates such as glucose and fructose with promising *in vitro* cytotoxicities against HeLa human cervical cancer and HCT116 human colon carcinoma cells [34,37]. The cytotoxicity of these complexes was found to be significantly influenced by the nature of the carbohydrate moiety and the metal center. Interestingly, iron complexes of the same ligands induced less cytotoxicity in cancer cells compared to the corresponding ruthenium complexes, confirming the importance of the ruthenium metal for the anticancer activity of such metallodrugs [34]. Valente et al. reported Ru(II)Cp complexes with the ability to induce inhibition of proliferation and apoptosis, not only in an estrogen receptor positive (ER +) breast cancer cell line (MCF7), but also in an aggressive triple negative breast cancer (TNBC) cell line (MDA-MB-231). These compounds were found to interact with mitochondria and with cytoskeleton, and to reduce the colony formation potential of breast cancer cells [46]. It is of high importance that Ru(II)Cp complexes display promising activities for the treatment of TNBC which, in contrast to hormone receptor positive (HR+) breast cancers, does not respond to hormonal therapy approaches [48,49]. DNA interaction [30,35,39], cell-membrane transporter inhibition [40], human serum albumin (HSA) binding [36] and cell cycle disturbance [39] have been also reported as other possible modes of action for Ru(II)Cp complexes. Ru(III) complexes have also attracted interest due to their cytotoxicity or/and antimetastatic properties alongside their low systemic toxicity [7,15,50]. For instance, the ruthenium (III) complex KP1339 did not only show cytotoxicity in different *in vivo* tumor models (more specifically in colon cancer) in preclinical studies, but was also found to stabilize the disease in clinical studies involving cancer patients while only inducing mild side effects. Disruption of endoplasmic reticulum homeostasis and induction of immunogenic cell death have been reported as mechanisms of action for this complex [15]. In the present study, we report the synthesis, characterization and stability assessment of Ru(II)COD, Ru(II)Cp, and Ru(III) complexes bearing anastrozole (ATZ) or letrozole (LTZ). Results regarding the *in vitro* anticancer activity in several human cell lines and *in vivo* toxicity in a zebrafish model of the most promising candidate is also presented.

2. Results and discussion

The synthesis of complex **1**, $RuCOD(ATZ)_2Cl_2$, was first attempted by allowing $[Ru(COD)Cl_2]_n$ to react with two equivalents of anastrozole in refluxing acetonitrile. No product could be detected after 18 h, and only a 13% conversion could be observed after 48 h. The yield could be increased up to 22% and the reaction time decreased to 25 min when the reaction was performed in a microwave reactor (15 psi, 200 W, 80 °C) (Scheme 1). It is noteworthy that using the microwave for longer periods of time under the above-mentioned conditions resulted in a significant decrease in the yield of the reaction, possibly due to some interactions of the final product with other molecules present in the reaction mixture. Only few examples of microwave-assisted syntheses of ruthenium complexes were previously reported [51–53]. The synthesis of cationic complex **2**, $RuCp(PPh_3)_2(ATZ)BF_4$, was performed by reacting $RuCp(PPh_3)_2Cl$ and anastrozole in the presence of $AgBF_4$ in refluxing acetone for 2 h (36% yield, Scheme 1). Both Ru(II) complexes **1** and **2** are soluble in acetone, alcohols and dimethyl sulfoxide (DMSO) but poorly soluble in water. The anionic Ru(III) species **3**, Na[*trans*-$RuCl_4ATZ(DMSO)$], was also prepared by allowing Na[*trans*-$RuCl_4(DMSO)_2$] to react with anastrozole in acetone overnight at room temperature (56% yield). Keeping in mind that the anticancer properties of metal complexes often vary with their lipophilicity [27,54], the sodium counterion in the structure of **3** was replaced with a more lipophilic cation. Complex **5**, PPh_4[*trans*-$RuCl_4ATZ$ (DMSO)], was then obtained (70% yield) by allowing a methanol solution of compound **3** to react with PPh_4Cl for 4 h at room temperature (Scheme 1). Although anastrozole and letrozole both belong to the third-generation class of aromatase inhibitors and have closely related structures, their efficacy has been reported to differ in some cases. For instance, letrozole was

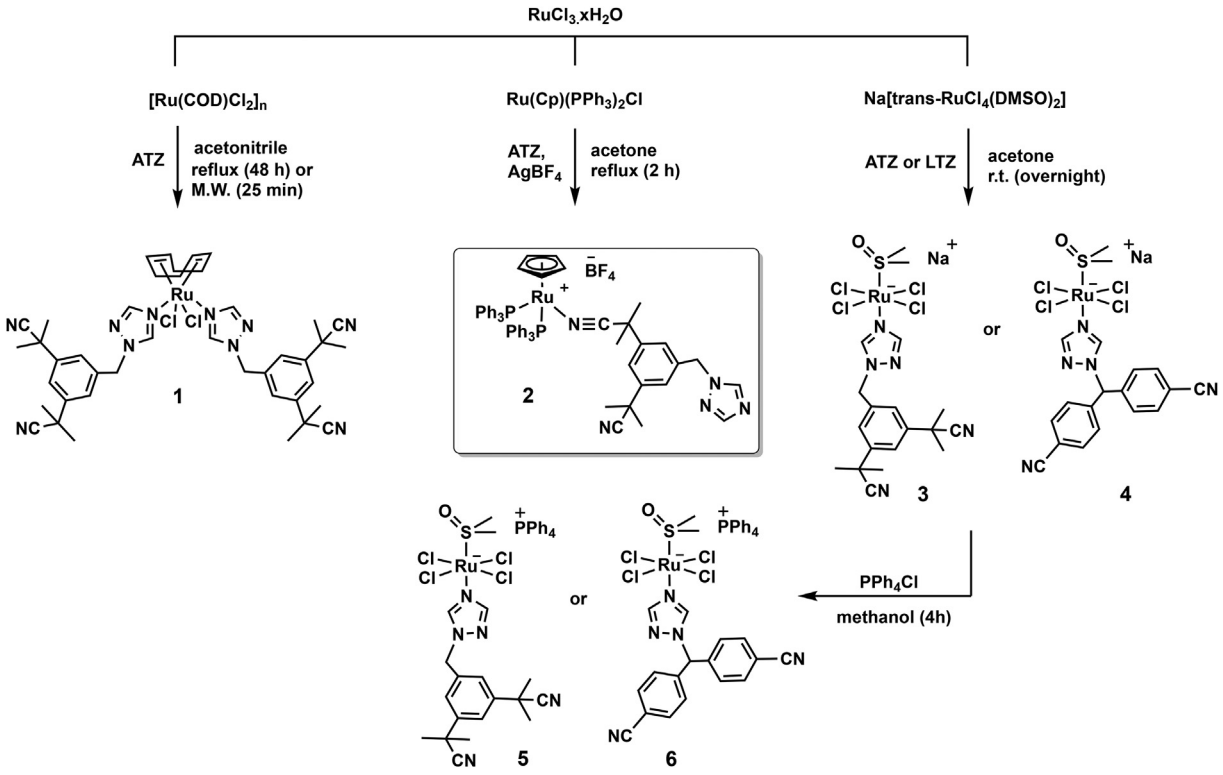

Scheme 1. Synthetic route to complexes **1**–**6**.

more effective at lowering estrogen levels than anastrozole in human breast cancer tissues [55,56]. For comparison purposes, letrozole derivatives of complexes **3** and **5**, **4** (66% yield) and **6** (39% yield), were also synthesized using the same reaction conditions (Scheme 1). All Ru(III) complexes were soluble in most organic solvents except **6** which had a poor solubility in most solvents. Due to the nature of the counterions, only complexes **3** and **4** were found to be soluble in water. The identity and purity of all complexes were confirmed by nuclear magnetic resonance (NMR) (only in the case of diamagnetic species **1** and **2**), high-resolution electrospray ionization mass spectrometry (HR-ESI-MS) and elemental analysis. In contrast to complex **1** and previously reported Ru(II) arene complexes bearing anastrozole or letrozole [16,26], signals corresponding to the protons and/or carbons of the anastrozole moiety in the ^{1}H NMR and ^{13}C{^{1}H} NMR spectra of **2** were non-equivalent (phenyl, nitrile and methyl groups), suggesting a different coordination mode of this ligand in this complex. Compared to the downfield chemical shift of ^{1}H NMR signals assigned to the protons of the triazole ring of **1**, the corresponding signals in the spectrum of **2** were only slightly shifted in comparison with the ones observed for free anastrozole (Fig. 1), suggesting that anastrozole is coordinated to ruthenium via one of its nitrile moieties, which was further confirmed by X-ray crystallography analysis (Fig. 2, *vide infra*). This mode of coordination may be favored due to the steric hindrance of the two bulky triphenylphosphine ligands, preventing the triazole ring from reaching the metal site. As reported for other Ru(II)Cp and Ru(II)COD complexes [30,57], a singlet at 4.51 ppm was observed for the cyclopentadienyl moiety of **2**, whereas three signals at 2.06, 2.66, 4.09 ppm were observed for the non-equivalent protons in of the cyclooctadienyl moiety of **1** (endo CH_2, exo CH_2 and CH).

The solid-state structure of all compounds (except **3**) was also confirmed by single crystal X-ray diffraction (Fig. 2 and Table S1). The six-coordinate metal center in **1** exhibits a distorted octahedral geometry. The Ru–C bond lengths are similar to those reported for other Ru(II)COD complexes [33,58,59]. The two chloride ligands *trans* to one another are directed away from the 1,5-COD ligand (the Cl1–Ru1–Cl2 bond angle is 159.95 (2)°), a common distortion found for ligands axial to an equatorial plane containing 1,5-COD in ruthenium (II) complexes [33,58,59]. The two anastrozole ligands are *cis* to one another (N1–Ru1–N2 89.87 (6)°) and *trans* to 1,5-COD. Compound **2** adopts a piano stool geometry, which is typical of cationic half-sandwich ruthenium complexes [34,39]. As previously stated, X-ray analysis data obtained for this complex confirmed the coordination of the anastrozole through one of its nitrile moieties. To the best of our knowledge, this is the first example of this coordination mode for a ruthenium complex bearing anastrozole. The Ru–N bond length in **2**, 2.048 (3) Å, is in the same range as bond lengths reported for other nitrile-coordinated Ru(II)Cp complexes (2.056 (3) Å [60] and 2.053 (2) Å [61]) and Ru(II)-arene complexes (2.066 (4) Å [62] and 2.050 (4) Å [63]), but as expected, significantly shorter than the ones noted for **1** (Ru–N1:2.136 (1) Å and Ru–N2: 2.133 (1) Å) and for previously reported Ru(II)-arene complexes of triazole-coordinating anastrozole [26]. The crystallography data for **4**–**6** also revealed a disordered octahedral geometry, which is well documented and characteristic for this type of Ru(III) complexes [64–67]. All the synthesized Ru(III) species include four chloride ligands in the equatorial positions and a DMSO molecule bound via its sulfur atom *trans* to the triazole ring of anastrozole or letrozole in the axial position. The Ru–N bond lengths observed in the structure of all Ru(III) species are very similar to one another (Ru–N: **4**, 2.091 (2); **5**, 2.103 (2); **6**, 2.093 (3)) and to those reported for structurally similar complexes [67,68]. The bond lengths and angles are also similar to those found in other NAMI-A derivatives [65–68].

DMSO was selected to prepare stock solutions of the compounds to assess their biological activity. DMSO is commonly used as a solvent of choice for this purpose as it allows the biological

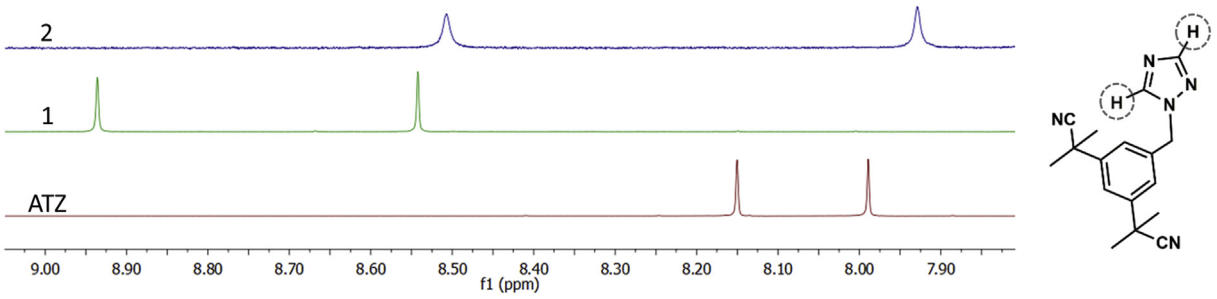

Fig. 1. Selected area of the ^{1}H NMR spectra of free anastrozole (red), complex **1** (green) and complex **2** (blue) in $CDCl_3$, showing the resonances corresponding to their triazole protons. (For interpretation of the references to colour in this figure legend, the reader is referred to the Web version of this article.)

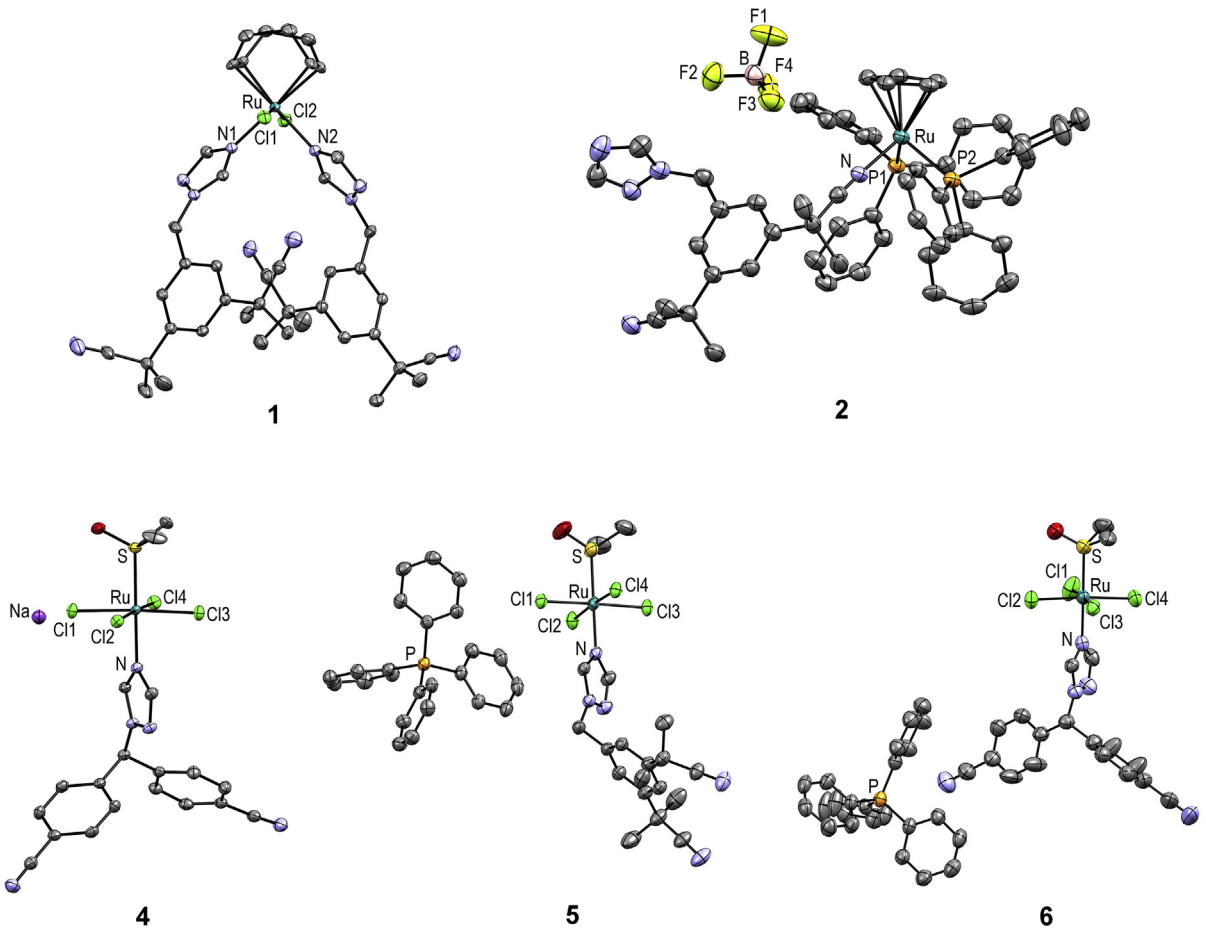

Fig. 2. ORTEP diagrams of **1**, **2** and **4**–**6** with thermal ellipsoids drawn at the 50% probability level. Note that only one site is shown for the disordered dimethyl sulfoxide molecule in the asymmetric unit of **6**, whereas two co-crystallized molecules of water in the asymmetric unit of **2** are omitted for clarity.

evaluation of compounds with poor aqueous solubility and does not induce noticeable *in vitro* or *in vivo* cytotoxicity at low concentrations. Prior to performing biological experiments, the solubility of the complexes in DMSO was estimated by measuring the UV–Vis absorbance of solutions of various concentrations after fine filtration. All complexes were found to be soluble in DMSO at concentrations as high as 20 mM, except complex **6** for which the biologically activity was not assessed. The stability of the complexes in DMSO (2 mM, 15 min) was also evaluated by NMR spectroscopy (only for the diamagnetic species). Whereas the ^{1}H NMR spectrum of complex **2** revealed its high stability in DMSO (only 2% of free anastrozole was observed) (Fig. S1), the ^{1}H NMR spectrum of compound **1** revealed a much lower stability in this solvent. Although the ^{1}H NMR spectrum of **1** (Fig. S1) indicated that **1** remained the major species in solution, the appearance of two new series of peaks corresponding to free anastrozole (25%) and a new complex bearing anastrozole discouraged us from pursuing the biological activity assessment of compound **1**. The stability of **2** in DMSO was further confirmed by UV–Vis spectrometry experiments. No apparent change was observed in the absorption spectrum of this compound over 1 h (Fig. S2).

To further investigate the stability of **2**–**5** under conditions similar to those of the tritiated water-release assay of aromatase activity, a previously established HPLC technique [26] was used,

allowing the measurement of the amount of released anastrozole or letrozole after a 1.5 h incubation of the complexes in full DMEM/F12 medium (with a maximum 0.1% DMSO) at 10 μM. Whereas all three Ru(III) complexes underwent transformation(s) in media, resulting in a significant release of their ligands (Table S2), compound **2** was found to be highly stable under the conditions tested (only 4% of released anastrozole was detected). Since complex **2** was the only species found to be stable under biologically relevant conditions, its solubility was verified by UV−Vis spectrometry under conditions similar to those used for the *in vitro* and *in vivo* experiments: *i)* in full DMEM/F12 medium (0.1% DMSO) and *ii)* in water (max 0.5% DMSO), respectively (Fig. S3). Compound **2** was found to be highly soluble at all tested concentrations (up to 15 μM in water and up to 20 μM in culture medium), confirming the suitability of this compound for biological experiments.

The cytotoxicity of complex **2** was evaluated at different concentrations using a sulforhodamine B (SRB) assay [69] in different human cell lines: MCF7 and T47D (ER + breast cancer), MDA-MB-231 (ER - breast cancer), H295R (adrenocortical carcinoma which expresses high levels of the aromatase enzyme) and MCF12A (non-cancerous breast) [70,71]. IC_{50} values were determined after a 48 h exposure of the cancer cells to the complex (Table 1).

In contrast to anastrozole alone (IC_{50} > 100 μM in all cell lines, results not shown), compound **2** displayed a high cytotoxicity against all the cancer cell lines with IC_{50} values lower than 1 μM. Although complex **2** approximately equally affected the healthy cell line tested with a selectivity index of 1.16, it is important to keep in mind that *i*) the same *in vitro* lack of selectivity was also observed for the widely used chemotherapeutic drug cisplatin (SI ≪ 1 in case of T47D and H295R cells) and that *ii*) although considered as an acceptable indicator, the *in vitro* cytotoxicity of a compound does not necessarily reflect its acute systemic toxicity and as a consequence, *in vivo* toxicities cannot be predicted from *in vitro* experiments with high confidence [72−74]. Importantly, complex **2** was more cytotoxic than cisplatin in all cancer cell lines used in this study, particularly in H295R and T47D cells (the latter being cisplatin resistant). Notably, compound **2** was not only found to be highly cytotoxic in ER + breast cancer cells (IC_{50} = 0.50 ± 0.09 μM, MCF7; 0.32 ± 0.03 μM, T47D) but also in a triple negative breast cancer (TNBC) cell line (IC_{50} = 0.39 ± 0.09 μM, MDA-MB-231), suggesting a mode of action that is independent of the estrogen receptor status of the cells. Indeed, it is of high importance to identify drug candidates for the treatment of aggressive hormone receptor negative (HR -, TNBC) breast cancers (about 10−20% of cases) for which endocrine therapies that target hormone receptors are ineffective [48,75]. The IC_{50} values observed for compound **2** are in the range expected for Ru(II)Cp complexes in both ER + breast cancer and TNBC cell lines (0.03−20 μM) [46,47,76−78], confirming the high potential of this class of ruthenium complexes for breast cancer treatment. Finally, compound **2** is a rare example of a ruthenium complex with significant cytotoxicity in H295R cells (IC_{50} = 0.63 ± 0.05 μM), warranting further investigations on the design of ruthenium species for the treatment of aggressive adrenocortical carcinomas. Nevertheless, it is important to keep in mind that *in vitro* cytotoxicity is not necessarily representative of *in vivo* antitumor activity, due to the potential impact of the tumor microenvironment on the tumor growth and drug effectiveness [79,80].

The binding of third generation aromatase inhibitors to the catalytic centre of the cytochrome P450 enzyme aromatase (CYP19A1) (consisting of an iron porphyrin complex) via their triazole nitrogen atom is considered to be their main mode of action [81]. Therefore, considering the availability of the triazole ring in the structure of **2**, we performed a molecular modeling study to evaluate the potential occurrence of interactions between this ruthenium complex and the enzyme using a docking simulation model we previously developed [26], based on the crystal structure of human placental aromatase cytochrome P450 (CYP19A1) (Fig. 3). These types of interactions between transition metal complexes and proteins (or DNA) were previously studied by other groups [82−84]. Molecular docking results suggest that bonding between the heme iron of CYP19 and triazole nitrogen atom is unlikely to occur. These results also reveal that significant conformational rearrangements of the protein would be required to accommodate compound **2** inside the active-site cavity of aromatase. Our simulations show that the interaction between **2** and the enzyme is energetically unfavorable because of significant steric clashes between compound **2** atoms and amino acids within the active-site cavity (Fig. 3C).

Table 1
IC_{50} values determined for **2** and cisplatin in human cancer MCF7, T47D, MDA-MB-231, H295R and non-cancerous MCF12A cell lines (and corresponding selectivity indexes).

	IC_{50} (μM)[a]		Selectivity index (SI)[b]	
	2	cisplatin	2	cisplatin
MCF7	0.50 (±0.09)	20.1 (±3.5)	1.16	2.12
T47D	0.32 (±0.03)	>150	1.81	<0.28
MDA-MB-231	0.39 (±0.09)	32.4 (±7.4)	1.49	1.32
H295R	0.63 (±0.05)	86.5 (±1.2)	0.92	0.49
MCF12A	0.58 (±0.02)	42.7 (±7.2)	–	–

[a] Inhibitory activity was determined by exposure of cell lines to each complex for 48 h and expressed as the concentration required to inhibit cell metabolic activity by 50% (IC_{50}). Errors correspond to the standard deviation of two to four independent experiments.
[b] SI= IC_{50} (non-cancerous MCF12A cell line)/IC_{50} (cancer cell line).

In the absence of conformational rearrangements of aromatase, the bulkiness of **2** (bearing two sterically hindered triphenylphosphine ligands) would prevent this complex from passing through the solvent-accessible access channel, preventing it to reach the active site of aromatase. This was further supported by results obtained from a tritiated water-release experiment we performed to assess the *in vitro* aromatase inhibitory effect of **2**. This method was previously reported as a sensitive and reproducible technique for aromatase activity assessment [85,86]. The H295R cell line was selected for this study as it expresses high levels of the aromatase enzyme [70,87]. As we previously reported for the investigation of the aromatase activity of H295R cells exposed to ruthenium species [26], H295R cells were co-incubated with 1β-^{3}H- androstenedione and compound **2** (or anastrozole) for 1.5 h. The radioactivity of the tritium oxide produced from the conversion of the labeled androgen to its corresponding estrogen, catalyzed by the aromatase enzyme, was quantified and reported as an indication of aromatase activity (Fig. 4). Because of the high cytotoxicity of **2** in H295R cells (IC_{50} = 0.63 ± 0.05 μM), its potential aromatase inhibitory activity was assessed at concentrations no greater than 100 nM (compound **2** becomes slightly cytotoxic at 1 μM when incubated for 1.5 h). As predicted from the docking simulation, a significantly lower aromatase inhibitory activity was observed in cells exposed to **2** compared to those treated with free anastrozole. No significant inhibition of aromatase activity was observed for complex **2** up to 10 nM, whereas about 50% inhibition of enzyme activity was observed for anastrozole alone at 10 nM (Fig. 4). It is likely that the slight aromatase inhibitory activity observed for **2** at higher concentrations was a consequence of free anastrozole released from the complex (4%, Table S2) under the conditions of the assay, making it difficult to draw a clear conclusion about the aromatase inhibitory activity of the complex itself.

The in vivo toxicity of **2** was determined in a zebrafish embryo

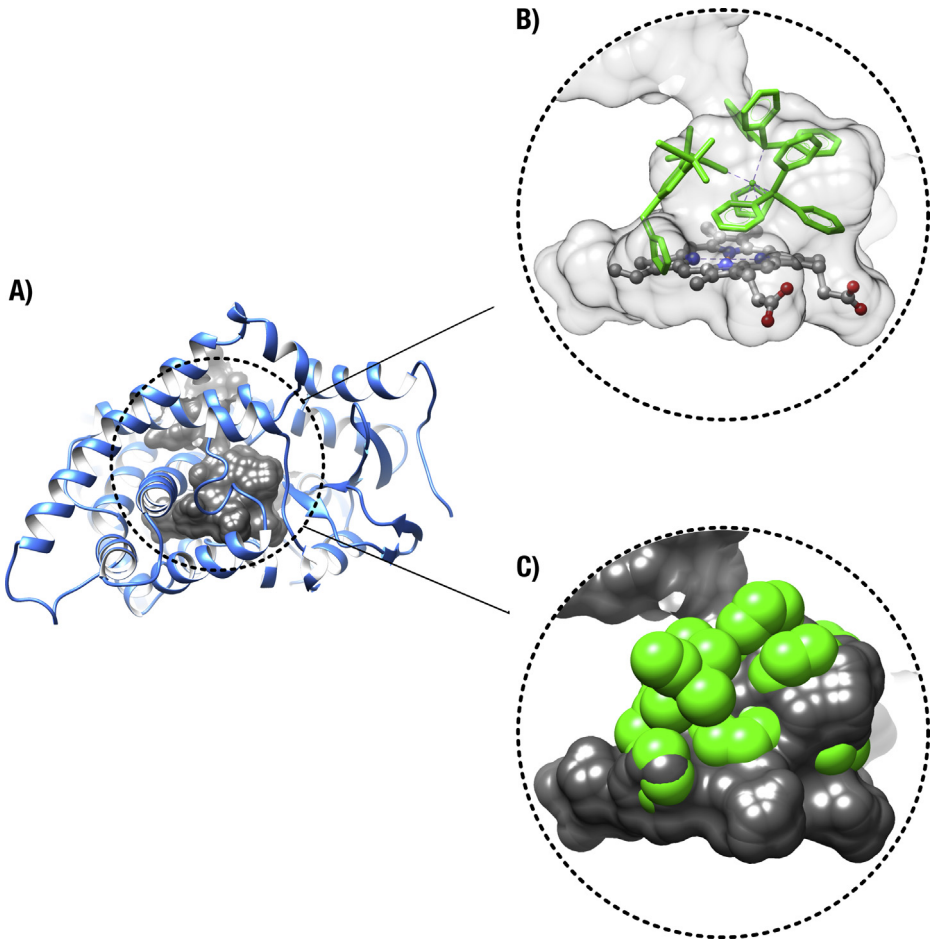

Fig. 3. Molecular docking of compound **2** inside the active-site cavity of aromatase. A) The active-site cavity of aromatase is shown in gray and the protein model is displayed as a blue ribbon. The illustrated surface represents the solvent-accessible area of the active site. B) Preferred conformer extracted for the ternary complex between the enzyme, cofactor group (heme), and compound **2**. The cofactor and compound **2** are respectively depicted as ball-and-stick and green stick models. C) Disruption of the internal cavity of the enzyme by compound **2**, illustrated as full atomic volume representation of van der Waals radii. Compound **2** atoms are shown as green spheres calculated according to the Corey-Pauling-Koltun model for van der Waals radii. Compound **2** atoms directly clash with amino acids within the active site of the enzyme, suggesting that such ternary complex formation is energetically unfavorable and nonspontaneous. (For interpretation of the references to colour in this figure legend, the reader is referred to the Web version of this article.)

model. Several publications support the use of this assay as a suitable model for the investigation of the *in vivo* toxicity of ruthenium species [26,27,88]. The zebrafish has become a prominent *in vivo* model in toxicology and drug discovery due to several advantages such as high fecundity (200−300 embryos per mating pair per week), ease of manipulation, embryo transparency, high degree of genetic conservation with humans and low cost [88−90]. Importantly, results arising from zebrafish toxicity screenings have been used as prediction tools prior to undertaking preclinical and clinical studies [91]. Accordingly, mortality rates, hatching rates and phenotype changes of zebrafish embryos exposed to **2** at concentrations around its IC_{50} value (0.1 μM, 0.5 μM and 1 μM) for *in vitro* cytotoxicity in human cancer cells were determined at 24, 48, 72 and 96 h post fertilization (hpf) (Fig. 5). Compared to untreated control embryos, no apparent mortality (data not shown), hatching delay or phenotype changes were observed in zebrafish embryos treated with **2** at the tested concentrations. It is noteworthy that we have previously reported a significant inhibition of the hatching rate for zebrafish embryos exposed to cisplatin at concentrations far less than its IC_{50} value in human cancer cells [26,27]. There are also a few studies reported for which Ru(II)Cp complexes have been investigated for their overall toxicity in a zebrafish model [78,92,93]. Although different conditions have been used for these studies preventing us from making direct comparisons, signs of toxicity such as delayed hatching, mortality and abnormalities such as pericardial edema, yolk sac edema, curved tail and head malfunction have been observed for some of the reported Ru(II)Cp complexes at the tested concentrations. Thus, compound **2** could be considered a promising candidate for further *in vivo* investigations.

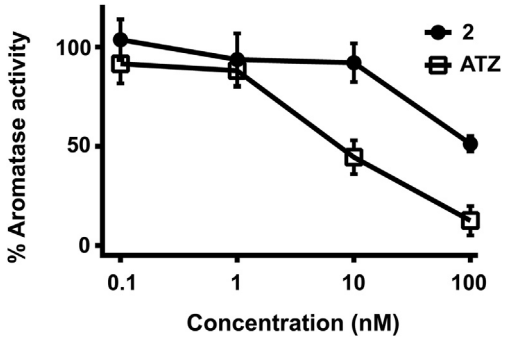

Fig. 4. Effects of the exposure of H295R cells to anastrozole (ATZ) and **2** on the aromatase activity. Cells were treated for 1.5 h with the indicated concentrations of the compounds. Values represent the mean ± SD.

3. Conclusion

From this study of a series of ruthenium complexes bearing anastrozole or letrozole (**1**–**6**), we observed that the solubility and the stability of the complexes can be highly affected by their type of backbone, the nature of their ligands or counterions and the type of coordination of their ligands. Our study clearly shows that Ru(II)Cp complex **2**, the only species in this series for which anastrozole is coordinated ruthenium through the nitrile moiety (and not via the nitrogen of the triazole ring), was the only complex found to be stable in DMSO and in cell culture medium. Whereas Ru(II)Cp complexes have been overlooked for their anticancer properties compared to their Ru(II) arene counterparts, *in vitro* and *in vivo* investigations of **2** confirm the high potential for this type of complexes for cancer therapy. Furthermore, results from the aromatase inhibition assay and the molecular docking simulation suggest that the bulkiness of a ruthenium complex such as **2** can be a factor preventing its interaction with the targeted enzyme, and that bulky moieties such as PPh_3 may not be ligands of choice for that purpose. Moreover, this study opens the door to the development of a novel class of Ru(II)Cp complexes for breast cancer therapy, particularly against TNBCs which respond poorly to existing chemotherapeutic agents.

4. Experimental section

General comments. All reagents were purchased from commercial sources and used without further purification. Experiments were performed under a nitrogen atmosphere using standard Schlenk techniques, and solvents were dried using a solvent purification system (Pure Process Technology). Anastrozole and letrozole were purchased from Triplebond and AK scientific, respectively. $RuCl_3.xH_2O$, 5-cyclooctadiene, dicyclopentadiene, triphenylphosphine, and silver tetrafluoroborate were purchased from Sigma Aldrich. $[Ru(COD)Cl_2]_n$ [94], $RuCp(PPh_3)_2Cl$ [95], and Na[*trans*-$RuCl_4(DMSO)_2$] [96] were prepared according to previously reported procedures. Tecan Infinite M1000 PRO microplate reader was used to read the absorbance of multiwell plates (at 510 nm) for SRB assay. NMR spectra (^1H, $^{13}C\{^1H\}$, COSY, HSQC, and ROESY) were recorded on a 400 MHz Varian or 600 MHz Bruker Avance III NMR spectrometers. Chemical shifts (δ) and coupling constants are expressed in ppm and Hz, respectively. ^1H and $^{13}C\{^1H\}$ spectra were referenced to solvent resonances, and spectral assignments were confirmed by 2D experiments. The purity of all ruthenium complexes (>95%) was assessed by elemental analyses (Laboratoire d'Analyze Élémentaire, Department of Chemistry, Université de Montréal). High-resolution and high accuracy mass spectra (HR-ESI-MS) were obtained using an Exactive Orbitrap spectrometer from ThermoFisher Scientific (Department of Chemistry, McGill University). Diffraction measurements were performed on a SMART APEX II diffractometer equipped with a CCD detector, an Incoatec IMuS source (Cu) and a Quazar MX mirror (**1** and **2**) or a Bruker Venture diffractometer (a liquid Ga Metal Jet source) equipped with a Photon 100 CMOS detector, a Helios MX optics and a Kappa goniometer (**4**–**6**) (Department of Chemistry, Université de Montréal). All statistical analyses were done using the GraphPad Prism 6.01 software. ANOVA analysis was used for testing the significance of the difference between the means and a p-value <0.05 was considered statistically significant.

4.1. Complex synthesis and characterization

$RuCOD(ATZ)_2Cl_2$ (1). Acetonitrile (18 mL) was added to anastrozole (0.208 g, 0.71 mmol), and $[Ru(COD)Cl_2]_n$ (0.100 g, 0.35 mmol). The mixture was heated under reflux for 48 h and then cooled to room temperature and filtered. The filtrate was evaporated to dryness and the crude yellow compound was purified by flash chromatography (silica gel) with ethyl acetate:hexane (4:1) as the mobile phase. Compound **1** (0.020 g, 13%) was obtained as a light-yellow precipitate. **Microwave-assisted synthesis.** A mixture of $[Ru(COD)Cl_2]_n$ (0.05 g, 0.18 mmol) and anastrozole (0.104 g, 0.36 mmol) in acetonitrile (10 mL) was heated in a microwave reactor at 80 °C for 25 min (set points: pressure 15 psi, power 200 W). The solvent was removed under vacuum and a light-yellow color product (0.034 g, 22%) was obtained after purification by column chromatography as mentioned above.^1H NMR ($CDCl_3$, 600 MHz): δ 1.71 (s, CH_3, 24H), 2.06 (m, C_8H_{12}, 4H), 2.66 (br, C_8H_{12}, 4H), 4.09 (br, C_8H_{12}, 4H), 5.34 (s, CH_2, 4H), 7.26 (d, J = 1.9 Hz, Ar*H*, 4H), 7.49 (t, J = 1.7 Hz, Ar*H*, 2H), 8.53 (s, $H_{triazole}$, 2H), 8.93 (s, $H_{triazole}$, 2H). $^{13}C\{^1H\}$ NMR ($CDCl_3$, 100 MHz): δ 29.04 (*s*), 30.05 (*s*), 37.30 (*s*), 53.82 (*s*), 89.53 (*s*), 122.02 (*s*), 123.76 (*s*), 124.25 (*s*), 135.87 (*s*), 143.4 (*s*), 145.15 (*s*), 151.92 (*s*). Found (%): C, 57.94; H, 5.83; N, 15.92. $C_{42}H_{50}Cl_2N_{10}Ru_1$ requires C, 58.17; H, 5.82; N, 16.16. HR-ESI-MS m/z (+): found 889.25 $[M + Na]^+$ (calc. 889.25).

$RuCp(PPh_3)_2(ATZ)BF_4$ (2). To a suspension of $RuCp(PPh_3)_2Cl$ (0.200 g, 0.276 mmol) in acetone (20 mL) were added anastrozole (0.164 g, 0.558 mmol) and $AgBF_4$ (0.060 g, 0.308 mmol). The solution was refluxed for 2 h until the colour changed from orange to pale yellow. The solution was centrifuged and the supernatant was evaporated under vacuum. The residue was dissolved in 2 mL of dichloromethane and was passed through a Celite pad. Diethyl ether was added to the filtrate and the resulting precipitate was

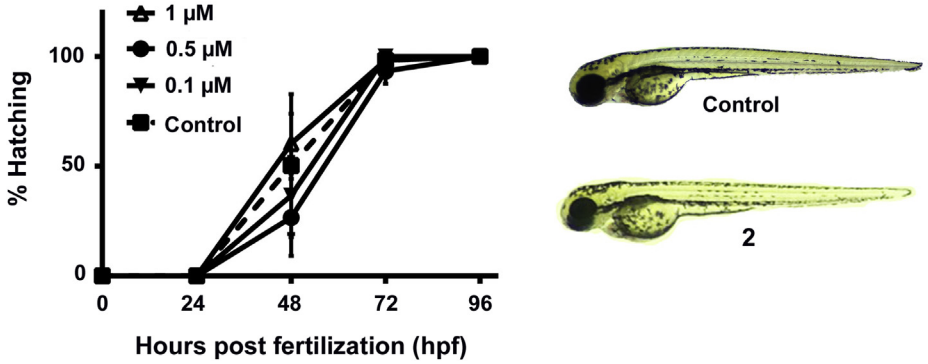

Fig. 5. (A) Effect of **2** on the hatching rate of developing zebrafish embryos. Hatching rates were assessed at 0.1, 0.5 and 1 µM over 4 days post fertilization (96 hpf). Control hatching rates are shown as a dashed line. (B) Gross morphological phenotypes of zebrafish embryos: untreated (control) and treated with 1 µM of **2** (96 hpf). Results are expressed as means ± standard deviation of three independent experiments (a total of 60 embryos).

washed with ethyl acetate (3 × 10 mL) and diethyl ether (3 × 10 mL). Compound **2** (0.107 g, 36%) was obtained as a pale-yellow precipitate. ^{1}H NMR ($CDCl_3$, 600 MHz): δ 1.42 (s, C*H*$_3$, 6H), 1.70 (s, C*H*$_3$, 6H), 4.51 (s, C$_5$*H*$_5$, 5H), 5.51 (s, C*H*$_2$, 2H), 7.00 (m, *H*$_{PPh3}$, 12H), 7.17 (t, J = 7.16 Hz, *H*$_{PPh3}$, 12H), 7.33 (t, J = 7.17 Hz, *H*$_{PPh3}$, 6H), 7.39 (t, J = 1.76, Ar*H*, 1H), 7.47 (s, Ar*H*, 1H), 7.73 (s, Ar*H*, 1H), 7.97 (s, *H*$_{triazole}$, 1H), 8.60 (s, *H*$_{triazole}$, 1H). ^{13}C{^{1}H} NMR ($CDCl_3$, 100 MHz): δ 27.65 (*s*), 29.13 (*s*), 37.50 (*s*), 39.39 (*s*), 52.47 (*s*), 83.80 (*s*), 121.66 (*s*), 124.34 (*s*), 124.91 (*s*), 126.26 (*s*), 128.39 (*t*), 130.13 (*s*), 133.06 (*t*), 135.75 (t), 136.21 (s), 138.28 (s), 141.38(s), 142,95(s), 144.38 (*s*), 152.10 (*s*). ^{31}P{^{1}H} NMR ($CDCl_3$, 200 MHz): δ 41.50. Found (%): C, 62.40; H, 5.23; N, 6.21. $C_{58}H_{54}BF_4N_5P_2Ru{\cdot}5/2H_2O$ requires C, 62.42, H 5.33, N 6.28. HR-ESI-MS m/z (+): found 984.29 M^+ (calc. 984.29), 691.13 $[M^+\text{-ATZ}]^+$ (calc. 691.13).

Na[*trans*-RuCl$_4$L(DMSO)] (L = ATZ, 3; L = LTZ, 4). Na [*trans*-$RuCl_4(DMSO)_2$] (0.36 mmol, 0,150 g) and L (1.08 mmol, L = ATZ: 0.315 g; L = LTZ: 0.303 g) were dissolved in acetone (10 mL) and the reaction was carried out overnight. The solution was evaporated to dryness and the crude compound was purified by flash chromatography (silica gel) with dichloromethane:methanol (20:1) as the mobile phase. **3** and **4** were obtained as light-yellow precipitates (**3**: 0.128 g, 56%; **4**: 0.149 g, 66%). **3**: Found (%): C, 35.02; H, 4.22; N, 10.65; S, 5.38. $C_{19}H_{25}Cl_4N_5NaORuS{\cdot}½H_2O$ requires C, 35.29; H, 4.06; N, 10.84; S, 4.95. HR-ESI-MS m/z (−): found 614.96 M^- (calc. 614.96)**;** **4**: Found (%): C, 35.50; H, 3.15; N, 10.55, S, 4.85. $C_{19}H_{17}Cl_4N_5NaORuS.H_2O$ requires C, 35.25; H, 2.96; N, 10.82; S, 4.95. HR-ESI-MS m/z (−): found 606.89 M^- (calc. 606.89).

PPh$_4$[*trans*-RuCl$_4$L(DMSO)] (L = ATZ, 5; L = LTZ, 6). PPh_4Cl (1.25 mmol, 470 mg) was added to a solution of **3** (0.125 mmol, 80 mg) or **4** (0.125 mmol, 79 mg) in methanol (8 mL) and the reaction was stirred at ambient temperature for 4 h. The solution was filtered, and the filtrate was dried under vacuum. The residue was washed by distilled water (4 × 20 mL) and diethyl ether (2 × 10 mL). Compounds **5** and **6** were obtained as yellow powders (**5**: 0.083 g, 69.6%; **6**: 0.045 g, 38.6%). **5**: Found (%): C, 53.66; H, 4.83; N, 7.24; S, 3.96. $C_{43}H_{45}Cl_4N_5OPRuS{\cdot}½\ H_2O$ requires C, 53.63; H, 4.82; N, 7.28; S, 3.32. HR-ESI-MS m/z (−): found 614.96 M^- (calc. 614.96), m/z (+): found 339.13 X^+ (calc. 339.13); **6**: Found (%): C, 54.24; H, 3.97; N, 7.35, S, 3.36. $C_{43}H_{37}Cl_4N_5OPRuS{\cdot}H_2O$ requires C, 54.60; H, 3.95; N, 7.41; S, 3.38. HR-ESI-MS m/z (−): found 606.89 M^- (calc. 606.89), m/z (+): found 339.13 X^+ (calc. 339.13).

Solubility in DMSO, media/DMSO, water/DMSO. UV−vis spectroscopy was used to evaluate the solubility of **1**–**6** in DMSO. Accordingly, solutions of **1**–**6** at different concentrations (5, 10, 15, 20 mM) were prepared in DMSO. The solutions were filtered using a short Celite pad and were then diluted 10 times in DMSO prior to UV−Vis measurements. The solubility of **2** was also investigated in phenol red free DMEM-F12 (DMSO 0.1%) at 0.01, 0.1, 1, 5, 10, 20 μM and in water (max DMSO 0.5%) at 1, 5, 10, 15 μM. All solutions were filtered (using a 0.2 μm syringe filter) prior to the UV−Vis measurements and the absorbance (350 nm−370 nm) was recorded using a microplate reader. The linearity between concentration and absorbance was considered as an indication of the solubility of the compounds at the desired concentrations. It is important to note that no supplementary technique was used here to evaluate if nanoaggregates were formed under these conditions.

Stability in cell culture media/DMSO. A previously developed HPLC-UV method [26] was used to measure the anastrozole (or letrozole) release in cell culture media supplemented with 0.1% DMSO. Stock solutions (10^4 μM) of **2**–**5** were prepared in DMSO. 10 μM solutions of the compounds were prepared by adding 20 μL of a stock solution to 20 mL of DMEM/F12. Solutions were incubated at 37 °C for 1.5 h, and further steps were achieved as described previously [26]. Briefly, after incubation, anastrozole or letrozole was retrieved from the media solution by liquid/liquid extraction using diethyl ether. After evaporation of the diethyl ether and after dissolving the residue in 2 mL of acetone, the solution was passed through a thin layer of silica (using 20 mL of acetone) to completely recover anastrozole (or letrozole) while minimizing the amount of undesired media residue in the final HPLC samples. Acetone was evaporated to dryness and the residue was dissolved in 1 mL of HPLC grade acetone containing 100 μM hydrocortisone as an external standard. The HPLC sample was injected into an Agilent UHPLC system (1260 Infinity GPC/SEC) using an Agilent Poroshell 120 EC-C18 column (4.6 × 100 mm, 2.7 μm) through a 13 min gradient of a mixture of acetonitrile and water at a flow rate of 2 mL/min: (a) 0−1 min, water, 100%; (b) 1−4 min, acetonitrile, 0−30%; (c) 4−10 min, acetonitrile, 30%; (d) 10−11 min, acetonitrile, 30%−100%; 11−13 min, acetonitrile, 100%. UV absorbance was acquired at 215 and standard curves of anastrozole and letrozole as the ones reported before [26] were used to quantify the amount of the aromatase inhibitors. All the experiments were carried out in three replicates.

X-ray diffraction analysis. Single crystals suitable for X-ray analysis were obtained by the room temperature slow evaporation of solutions of **1** (in ethyl acetate), **4** (in methanol), **5** (in dichloromethane), and **6** (in dichloromethane/diethyl ether). Single crystals of **2** were obtained from an ethyl acetate solution kept at 4 °C for two weeks. Cell refinement and data reduction were done using APEX2. Absorption corrections were applied using SADABS. Structures were solved by direct methods using SHELXS-97 and refined on F^2 by full-matrix least squares using SHELXL-97 or SHELXL-2014. All non-hydrogen atoms were refined anisotropically, whereas hydrogen atoms were refined isotropic on calculated positions using a riding model [97−99].

Cell culture. All the protocols reported for biological studies were approved by the Institutional Research Ethics Committee of INRS − Centre Armand-Frappier Santé Biotechnologie. All cell culture products were obtained from commercial sources such as Gibco, Sigma Aldrich, Corning, and Invitrogen. RPMI 1640 supplemented with fetal bovine serum (10%) was used to culture human breast cancer MCF7 and MDA-MB-231 cell lines. Human breast cancer T47D cells were grown in RPMI 1640 supplemented with HEPES (2.38 g/L), sodium pyruvate (0.11 g/L), glucose (2.5 g/L), insulin bovine (10 μg/mL), and fetal bovine serum (10%). Adrenocortical carcinoma H295R cells were grown in DMEM/F-12 supplemented with Nu Serum (2.5%) and ITS (1%). MCF12A cells were maintained in phenol Dulbecco's modified Eagle's medium Ham's F12 (DMEM/F12) culture medium supplemented with 5% (v/v) horse serum, hEGF recombinant (20 ng/mL), hydrocortisone (500 ng/mL), and insulin (10 μg/mL). All growth media were supplemented with penicillin/streptomycin. Cells were propagated according to ATCC guidelines.

Sulforhodamine B (SRB) Assay. The cytotoxicity of **2**, anastrozole and cisplatin in MCF7, T47D, MDA-MB-231 and MCF12A cells were evaluated using the SRB assay. Cells were cultured in 96-well plates (10^4 cells/well) and incubated in 5% CO_2 at 37 °C overnight. Cells were treated with different concentrations of each compound, carrier (media containing maximum 0.5% DMSO) and positive control (media containing 25% DMSO). The plates were incubated for 48 h and further steps were done as previously reported [26]. IC_{50} values were determined by the plots of viability versus concentration. Error bars were calculated as the standard error of three independent experiments.

Aromatase activity measurement. Aromatase activity was measured using a tritiated water-release assay. H295R cells that can express high level of aromatase enzyme *in vitro* [70] were cultured in 24-well plates (100,000 cells/well) containing 1 mL of DMEM/F-12 supplemented with Nu Serum and ITS and were incubated for 24 h. After removing the medium and washing cells with 500 μL

PBS, a volume of 250 μL of phenol red free DMEM/F-12 containing 54 nM 1β-^{3}H-androstenedione and different concentrations of anastrozole and **2** (0.1, 1, 10 and 100 nM) were added to each well, and cells were incubated for 1.5 h at 37 °*C* (5% CO_2). Further steps were performed as described previously [71]. Tritiated water in a liquid scintillation cocktail was counted using a Microbeta Trilux (PerkinElmer, Waltham, Massachusetts). Incubations in the absence of cells (blanks) and in the presence of DMSO 0.1% (which was the concentration used to dissolve the complexes in the growth media for this study) were included as controls.

Zebrafish embryo assay. Wild-type zebrafish (*Danio rerio*) embryos were raised at 28.5 °C and staged as previously described [100]. Embryos at the 2-cell or 4-cell stage were seeded in 6-well plates and exposed to 5 mL fish medium containing **2** at different concentrations (0.1, 0.5, 1 μM). Final concentration of DMSO in which the stock solutions were prepared was 0.5%. The mortality, gross morphology, and hatching rates of the zebrafish embryos without and with the desired compounds were observed every 24 h for a period of 96 h under a stereo microscope (Leika S6E). The medium (containing the compound to be tested) was refreshed after 48 h for each experiment. A no-treatment control was also included. Experiments were performed in triplicates, and a total of 60 embryos from the pooling of three different crosses have been used per each treatment. Zebrafish experiments were performed following a protocol approved by the Canadian Council for Animal Care (CCAC) and our local animal care committee.

Virtual docking of compound 2 to human aromatase. Human aromatase (PDB entry 5JL6) was previously solvated with water molecules using the YASARA minimization system and standard protocols [101]. Complex **2** was used as ligand and its structure was generated with the XT structure solution program and refined using a least squares minimization protocol [26]. Compound **2** was then used in combination with the heme group as cofactor and the energetically minimized aromatase structure, as previously described [26]. We used the cavity detection standard protocol incorporated in the Molegro Virtual Docker 6.0 suite as first step to identify and establish the active-site cavity of the enzyme. The best ternary complex solution for this compound was obtained after a 20-run simulation of 3,500 iteration cycles with an initial population of 100 conformers per iteration. The preferred conformer arose from a protocol that explored up to 7,000,000 combinations. The MolDock scoring function was used to score the best conformer solutions without the incorporation of solvent molecules [102]. USCF Chimera 1.1 was used for molecular structure visualization [45].

Accession Codes

CCDC 1962264–1962268 contain the supplementary crystallographic data for this paper. These data can be obtained free of charge via www.ccdc.cam.ac.uk/data_request/cif, or by emailing data_request@ccdc.cam.ac.uk, or by contacting The Cambridge Crystallographic Data Centre, 12 Union Road, Cambridge CB2 1EZ, UK; fax: +44 1223 336033.

Declaration of competing interest

The authors declare that they have no known competing financial interests or personal relationships that could have appeared to influence the work reported in this paper.

Acknowledgements

This work was supported by the Institut national de la recherche scientifique (INRS), the Natural Sciences and Engineering Research Council of Canada (NSERC) (A.C., J.T.S. and N.D.), the Fonds de Recherche du Québec Santé (FRQS) (A.C., S.A.P., N.D.), the Canadian Institutes of Health Research (CIHR) (S.A.P.), the Canada Foundation for Innovation (CFI) (A.C., S.A.P., and N.D.), the National Institutes of Health (NIH) (N.D.) and the Armand-Frappier Foundation (scholarship to G.G.). We would like to thank Prof. David Chatenet and Prof. Isabelle Plante for providing the human cancer cell lines used in this study, as well as Prof. Charles Ramassamy for providing access to his laboratory instrumentation.

Appendix A. Supplementary data

Supplementary data to this article can be found online at https://doi.org/10.1016/j.ejmech.2019.112030.

References

[1] C.S. Allardyce, P.J. Dyson, Metal-based drugs that break the rules, Dalton Trans. 45 (2016) 3201–3209.
[2] R.H. Berndsen, A. Weiss, U.K. Abdul, T.J. Wong, P. Meraldi, A.W. Griffioen, P.J. Dyson, P. Nowak-Sliwinska, Combination of ruthenium(II)-arene complex [Ru(η^6-p-cymene)Cl_2(pta)] (RAPTA-C) and the epidermal growth factor receptor inhibitor erlotinib results in efficient angiostatic and antitumor activity, Sci. Rep. 7 (2017) 43005.
[3] T.C. Johnstone, G.Y. Park, S.J. Lippard, Understanding and improving platinum anticancer drugs–phenanthriplatin, Anticancer Res. 34 (2014) 471–476.
[4] J. Li, L. Guo, Z. Tian, S. Zhang, Z. Xu, Y. Han, R. Li, Y. Li, Z. Liu, Half-sandwich iridium and ruthenium complexes: effective tracking in cells and anticancer studies, Inorg. Chem. 57 (2018) 13552–13563.
[5] D.S. Williams, G.E. Atilla, H. Bregman, A. Arzoumanian, P.S. Klein, E. Meggers, Switching on a signaling pathway with an organoruthenium complex, Angew. Chem. Int. Ed. 44 (2005) 1984–1987.
[6] K.S.M. Smalley, R. Contractor, N.K. Haass, A.N. Kulp, G.E. Atilla-Gokcumen, D.S. Williams, H. Bregman, K.T. Flaherty, M.S. Soengas, E. Meggers, M. Herlyn, An organometallic protein kinase inhibitor pharmacologically activates p53 and induces apoptosis in human melanoma cells, Cancer Res. 67 (2007) 209–217.
[7] E. Alessio, Thirty years of the drug candidate NAMI-A and the myths in the field of ruthenium anticancer compounds: a personal perspective, Eur. J. Inorg. Chem. 2017 (2017) 1549–1560.
[8] S. Leijen, S.A. Burgers, P. Baas, D. Pluim, M. Tibben, E. van Werkhoven, E. Alessio, G. Sava, J.H. Beijnen, J.H.M. Schellens, Phase I/II study with ruthenium compound NAMI-A and gemcitabine in patients with non-small cell lung cancer after first line therapy, Investig. New Drugs 33 (2015) 201–214.
[9] A.A. Holder, L. Lilge, W.R. Browne, M.A.W. Lawrence, J.L. Bullock, Ruthenium Complexes: Photochemical and Biomedical Applications, first ed., Wiley-VCH, 2017.
[10] H.A. Burris, S. Bakewell, J.C. Bendell, J. Infante, S.F. Jones, D.R. Spigel, G.J. Weiss, R.K. Ramanathan, A. Ogden, D. Von Hoff, Safety and activity of IT-139, a ruthenium-based compound, in patients with advanced solid tumours: a first-in-human, open-label, dose-escalation phase I study with expansion cohort, ESMO Open 1 (2016), e000154.
[11] S. Monro, K.L. Colón, H. Yin, J. Roque, P. Konda, S. Gujar, R.P. Thummel, L. Lilge, C.G. Cameron, S.A. McFarland, Transition metal complexes and photodynamic therapy from a tumor-centered approach: challenges, opportunities, and highlights from the development of TLD1433, Chem. Rev. 119 (2019) 797–828.
[12] A. Bergamo, C. Gaiddon, J.H.M. Schellens, J.H. Beijnen, G. Sava, Approaching tumour therapy beyond platinum drugs: status of the art and perspectives of ruthenium drug candidates, J. Inorg. Biochem. 106 (2012) 90–99.
[13] S. Thota, D.A. Rodrigues, D.C. Crans, E.J. Barreiro, Ru(II) compounds: next-generation anticancer metallotherapeutics? J. Med. Chem. 61 (2018) 5805–5821.
[14] S. Bonnet, Why develop photoactivated chemotherapy? Dalton Trans. 47 (2018) 10330–10343.
[15] D. Wernitznig, K. Kiakos, G. Del Favero, N. Harrer, H. Machat, A. Osswald, M.A. Jakupec, A. Wernitznig, W. Sommergruber, B.K. Keppler, First-in-class ruthenium anticancer drug (KP1339/IT-139) induces an immunogenic cell death signature in colorectal spheroids in vitro, Metallomics 11 (2019) 1044–1048.
[16] A. Castonguay, C. Doucet, M. Juhas, D. Maysinger, New ruthenium(II)–Letrozole complexes as anticancer therapeutics, J. Med. Chem. 55 (2012) 8799–8806.
[17] K.J. Kilpin, P.J. Dyson, Enzyme inhibition by metal complexes: concepts, strategies and applications, Chem. Sci. 4 (2013) 1410–1419.
[18] C. Mu, K.E. Prosser, S. Harrypersad, G.A. MacNeil, R. Panchmatia, J.R. Thompson, S. Sinha, J.J. Warren, C.J. Walsby, Activation by oxidation: ferrocene-functionalized Ru(II)-Arene complexes with anticancer, antibacterial, and antioxidant properties, Inorg. Chem. 57 (2018) 15247–15261.

[19] W.H. Ang, L.J. Parker, A. De Luca, L. Juillerat-Jeanneret, C.J. Morton, M. Lo Bello, M.W. Parker, P.J. Dyson, Rational design of an organometallic glutathione transferase inhibitor, Angew. Chem. Int. Ed. 48 (2009) 3854–3857.

[20] R.W. Brueggemeier, J.C. Hackett, E.S. Diaz-Cruz, Aromatase inhibitors in the treatment of breast cancer, Endocr. Rev. 26 (2005) 331–345.

[21] P.E. Goss, K. Strasser, Aromatase inhibitors in the treatment and prevention of breast cancer, J. Clin. Oncol. 19 (2001) 881–894.

[22] R. Jeselsohn, J.S. Bergholz, M. Pun, M. Cornwell, W. Liu, A. Nardone, T. Xiao, W. Li, X. Qiu, G. Buchwalter, A. Feiglin, K. Abell-Hart, T. Fei, P. Rao, H. Long, N. Kwiatkowski, T. Zhang, N. Gray, D. Melchers, R. Houtman, X.S. Liu, O. Cohen, N. Wagle, E.P. Winer, J. Zhao, M. Brown, Allele-specific chromatin recruitment and therapeutic vulnerabilities of ESR1 activating mutations, Cancer Cell 33 (2018) 173–186, e175.

[23] I.E. Krop, I.A. Mayer, V. Ganju, M. Dickler, S. Johnston, S. Morales, D.A. Yardley, B. Melichar, A. Forero-Torres, S.C. Lee, R. de Boer, K. Petrakova, S. Vallentin, E.A. Perez, M. Piccart, M. Ellis, E. Winer, S. Gendreau, M. Derynck, M. Lackner, G. Levy, J. Qiu, J. He, P. Schmid, Pictilisib for oestrogen receptor-positive, aromatase inhibitor-resistant, advanced or metastatic breast cancer (FERGI): a randomised, double-blind, placebo-controlled, phase 2 trial, Lancet Oncol. 17 (2016) 811–821.

[24] M. O'Neill, F.E.M. Paulin, J. Vendrell, C.W. Ali, A.M. Thompson, The aromatase inhibitor letrozole enhances the effect of doxorubicin and docetaxel in an MCF7 cell line model, BioDiscovery 6 (2012), e8940.

[25] A.A. Miranda, J. Limon, F.L. Medina, C. Arce, J.W. Zinser, E.B. Rocha, C.M. Villarreal-Garza, Combination treatment with aromatase inhibitor and capecitabine as first- or second-line treatment in metastatic breast cancer, J. Clin. Oncol. 30 (2012), e11016.

[26] G. Golbaghi, M.M. Haghdoost, D. Yancu, Y. López de los Santos, N. Doucet, S.A. Patten, J.T. Sanderson, A. Castonguay, Organoruthenium(II) complexes bearing an aromatase inhibitor: synthesis, characterization, in vitro biological activity and in vivo toxicity in zebrafish embryos, Organometallics 38 (2019) 702–711.

[27] M.M. Haghdoost, G. Golbaghi, M. Letourneau, S.A. Patten, A. Castonguay, Lipophilicity-antiproliferative activity relationship study leads to the preparation of a ruthenium(II) arene complex with considerable in vitro cytotoxicity against cancer cells and a lower in vivo toxicity in zebrafish embryos than clinically approved cis-platin, Eur. J. Med. Chem. 132 (2017) 282–293.

[28] M.M. Haghdoost, J. Guard, G. Golbaghi, A. Castonguay, Anticancer activity and catalytic potential of ruthenium(II)–Arene complexes with N,O-donor ligands, Inorg. Chem. 57 (2018) 7558–7567.

[29] J.P.C. Coverdale, I. Romero-Canelón, C. Sanchez-Cano, G.J. Clarkson, A. Habtemariam, M. Wills, P.J. Sadler, Asymmetric transfer hydrogenation by synthetic catalysts in cancer cells, Nat. Chem. 10 (2018) 347–354.

[30] V. Moreno, J. Lorenzo, F.X. Aviles, M.H. Garcia, J.P. Ribeiro, T.S. Morais, P. Florindo, M.P. Robalo, Studies of the antiproliferative activity of ruthenium (II) cyclopentadienyl-derived complexes with nitrogen coordinated ligands, Bioinorgan. Chem. Appl. 2010 (2010) 11.

[31] L. Côrte-Real, F. Mendes, J. Coimbra, T.S. Morais, A.I. Tomaz, A. Valente, M.H. Garcia, I. Santos, M. Bicho, F. Marques, Anticancer activity of structurally related ruthenium(II) cyclopentadienyl complexes, J. Biol. Inorg. Chem. 19 (2014) 853–867.

[32] B.T. Loughrey, P.C. Healy, P.G. Parsons, M.L. Williams, Selective cytotoxic Ru(II) arene cp* complex salts $[R\text{-}PhRuCp^*]^+X^-$ for X = BF_4^-, PF_6^-, and BPh_4^-, Inorg. Chem. 47 (2008) 8589–8591.

[33] S. Thangavel, R. Rajamanikandan, H.B. Friedrich, M. Ilanchelian, B. Omondi, Binding interaction, conformational change, and molecular docking study of N-(pyridin-2-ylmethylene)aniline derivatives and carbazole Ru(II) complexes with human serum albumins, Polyhedron 107 (2016) 124–135.

[34] P.R. Florindo, D.M. Pereira, P.M. Borralho, C.M.P. Rodrigues, M.F.M. Piedade, A.C. Fernandes, Cyclopentadienyl–Ruthenium(II) and iron(II) organometallic compounds with carbohydrate derivative ligands as good colorectal anticancer agents, J. Med. Chem. 58 (2015) 4339–4347.

[35] V. Moreno, M. Font-Bardia, T. Calvet, J. Lorenzo, F.X. Avilés, M.H. Garcia, T.S. Morais, A. Valente, M.P. Robalo, DNA interaction and cytotoxicity studies of new ruthenium(II) cyclopentadienyl derivative complexes containing heteroaromatic ligands, J. Inorg. Biochem. 105 (2011) 241–249.

[36] L. Côrte-Real, M.P. Robalo, F. Marques, G. Nogueira, F. Avecilla, T.J.L. Silva, F.C. Santos, A.I. Tomaz, M.H. Garcia, A. Valente, The key role of coligands in novel ruthenium(II)-cyclopentadienyl bipyridine derivatives: ranging from non-cytotoxic to highly cytotoxic compounds, J. Inorg. Biochem. 150 (2015) 148–159.

[37] P. Florindo, I.J. Marques, C.D. Nunes, A.C. Fernandes, Synthesis, characterization and cytotoxicity of cyclopentadienyl ruthenium(II) complexes containing carbohydrate-derived ligands, J. Organomet. Chem. 760 (2014) 240–247.

[38] T.S. Morais, A. Valente, A.I. Tomaz, F. Marques, M.H. Garcia, Tracking antitumor metallodrugs: promising agents with the Ru(II)- and Fe(II)-cyclopentadienyl scaffolds, Future Med. Chem. 8 (2016) 527–544.

[39] D. Mavrynsky, J. Rahkila, D. Bandarra, S. Martins, M. Meireles, M.J. Calhorda, I.J. Kovács, I. Zupkó, M.M. Hänninen, R. Leino, Cytotoxicities of polysubstituted chlorodicarbonyl(cyclopentadienyl) and (Indenyl)ruthenium complexes, Organometallics 32 (2013) 3012–3017.

[40] L. Côrte-Real, R.G. Teixeira, P. Gírio, E. Comsa, A. Moreno, R. Nasr, H. Baubichon-Cortay, F. Avecilla, F. Marques, M.P. Robalo, P. Mendes, J.P.P. Ramalho, M.H. Garcia, P. Falson, A. Valente, Methyl-cyclopentadienyl ruthenium compounds with 2,2′-bipyridine derivatives display strong anticancer activity and multidrug resistance potential, Inorg. Chem. 57 (2018) 4629–4639.

[41] C. Kasper, H. Alborzinia, S. Can, I. Kitanovic, A. Meyer, Y. Geldmacher, M. Oleszak, I. Ott, S. Wölfl, W.S. Sheldrick, Synthesis and cellular impact of diene–ruthenium(II) complexes: a new class of organoruthenium anticancer agents, J. Inorg. Biochem. 106 (2012) 126–133.

[42] N. Mendes, F. Tortosa, A. Valente, F. Marques, A. Matos, T.S. Morais, A.I. Tomaz, F. Gärtner, M.H. Garcia, In vivo performance of a ruthenium-cyclopentadienyl compound in an orthotopic triple negative breast cancer model, Anti Cancer Agents Med. Chem. 17 (2017) 126–136.

[43] B. Dutta, C. Scolaro, R. Scopelliti, P.J. Dyson, K. Severin, Importance of the π-ligand: remarkable effect of the cyclopentadienyl ring on the cytotoxicity of ruthenium PTA compounds, Organometallics 27 (2008) 1355–1357.

[44] G. Süss-Fink, Arene ruthenium complexes as anticancer agents, Dalton Trans. 39 (2010) 1673–1688.

[45] A.I. Tomaz, T. Jakusch, T.S. Morais, F. Marques, R.F.M. de Almeida, F. Mendes, É.A. Enyedy, I. Santos, J.C. Pessoa, T. Kiss, M.H. Garcia, $[RuII(\eta^5\text{-}C_5H_5)(bipy)(PPh_3)]^+$, a promising large spectrum antitumor agent: cytotoxic activity and interaction with human serum albumin, J. Inorg. Biochem. 117 (2012) 261–269.

[46] T. Moreira, R. Francisco, E. Comsa, S. Duban-Deweer, V. Labas, A.-P. Teixeira-Gomes, L. Combes-Soia, F. Marques, A. Matos, A. Favrelle, C. Rousseau, P. Zinck, P. Falson, M.H. Garcia, A. Preto, A. Valente, Polymer "ruthenium-cyclopentadienyl" conjugates - new emerging anti-cancer drugs, Eur. J. Med. Chem. 168 (2019) 373–384.

[47] T.S. Morais, T.J.L. Silva, F. Marques, M.P. Robalo, F. Avecilla, P.J.A. Madeira, P.J.G. Mendes, I. Santos, M.H. Garcia, Synthesis of organometallic ruthenium(II) complexes with strong activity against several human cancer cell lines, J. Inorg. Biochem. 114 (2012) 65–74.

[48] S. Al-Mahmood, J. Sapiezynski, O.B. Garbuzenko, T. Minko, Metastatic and triple-negative breast cancer: challenges and treatment options, Drug Deliv. Transl. Res. 8 (2018) 1483–1507.

[49] G. Bianchini, J.M. Balko, I.A. Mayer, M.E. Sanders, L. Gianni, Triple-negative breast cancer: challenges and opportunities of a heterogeneous disease, Nat. Rev. Clin. Oncol. 13 (2016) 674–690.

[50] R. Trondl, P. Heffeter, C.R. Kowol, M.A. Jakupec, W. Berger, B.K. Keppler, NKP-1339, the first ruthenium-based anticancer drug on the edge to clinical application, Chem. Sci. 5 (2014) 2925–2932.

[51] J. Cao, Q. Wu, W. Zheng, L. Li, W. Mei, Microwave-assisted synthesis of polypyridyl ruthenium(ii) complexes as potential tumor-targeting inhibitors against the migration and invasion of Hela cells through G2/M phase arrest, RSC Adv. 7 (2017) 26625–26632.

[52] F.A. Beckford, J.M. Shaloski, G. Leblanc, J. Thessing, L.C. Lewis-Alleyne, A.A. Holder, L. Li, N.P. Seeram, Microwave synthesis of mixed ligand diimine–thiosemicarbazone complexes of ruthenium(ii): biophysical reactivity and cytotoxicity, Dalton Trans. (2009) 10757–10764.

[53] T.J. Anderson, J.R. Scott, F. Millett, B. Durham, Decarboxylation of 2,2'-Bipyridinyl-4,4'-dicarboxylic acid diethyl ester during microwave synthesis of the corresponding trichelated ruthenium complex, Inorg. Chem. 45 (2006) 3843–3845.

[54] M.M. Haghdoost, G. Golbaghi, J. Guard, S. Sielanczyk, S.A. Patten, A. Castonguay, Synthesis, characterization and biological evaluation of cationic organoruthenium(ii) fluorene complexes: influence of the nature of the counteranion, Dalton Trans. 48 (2019) 13396–13405.

[55] J. Geisler, Differences between the non-steroidal aromatase inhibitors anastrozole and letrozole – of clinical importance? Br. J. Canc. 104 (2011) 1059–1066.

[56] J. Geisler, B. Haynes, G. Anker, M. Dowsett, P.E. Lønning, Influence of letrozole and anastrozole on total body aromatization and plasma estrogen levels in postmenopausal breast cancer patients evaluated in a randomized, cross-over study, J. Clin. Oncol. 20 (2002) 751–757.

[57] N. Bharti, M.R. Maurya, F. Naqvi, A. Azam, Synthesis and antiamoebic activity of new cyclooctadiene ruthenium(II) complexes with 2-acetylpyridine and benzimidazole derivatives, Bioorg. Med. Chem. Lett 10 (2000) 2243–2245.

[58] J.A. Widegren, H. Weiner, S.M. Miller, R.G. Finke, Improved synthesis and crystal structure of tetrakis(acetonitrile)(η^4-1,5-cyclooctadiene)ruthenium(II) bis[tetrafluoroborate(1−)], J. Organomet. Chem. 610 (2000) 112–117.

[59] J.J. Adams, A.S. Del Negro, N. Arulsamy, B.P. Sullivan, Unexpected formation of ruthenium(II) hydrides from a reactive dianiline precursor and 1,2-$(ph_2P)_2$-1,2-closo-$C_2B_{10}H_{10}$, Inorg. Chem. 47 (2008) 1871–1873.

[60] E.A. Nyawade, H.B. Friedrich, B. Omondi, H.Y. Chenia, M. Singh, S. Gorle, Synthesis and characterization of new α,α′-diaminoalkane-bridged dicarbonyl(η^5-cyclopentadienyl)ruthenium(II) complex salts: antibacterial activity tests of η^5-cyclopentadienyl dicarbonyl ruthenium(II) amine complexes, J. Organomet. Chem. 799–800 (2015) 138–146.

[61] E. Rüba, W. Simanko, K. Mauthner, K.M. Soldouzi, C. Slugovc, K. Mereiter, R. Schmid, K. Kirchner, $[RuCp(PR_3)(CH_3CN)_2]PF_6$ (R = ph, me, cy). Convenient precursors for mixed ruthenium(II) and ruthenium(IV) half-sandwich complexes, Organometallics 18 (1999) 3843–3850.

[62] J.-B. Sortais, N. Pannetier, A. Holuigue, L. Barloy, C. Sirlin, M. Pfeffer, N. Kyritsakas, Cyclometalation of primary benzyl amines by ruthenium(II), rhodium(III), and iridium(III) complexes, Organometallics 26 (2007) 1856–1867.

[63] S. Jung, K. Ilg, C.D. Brandt, J. Wolf, H. Werner, A series of ruthenium(ii) complexes containing the bulky, functionalized trialkylphosphines $^{t}Bu_2PCH_2XC_6H_5$ as ligands, J. Chem. Soc., Dalton Trans. (2002) 318–327.

[64] E. Alessio, G. Balducci, A. Lutman, G. Mestroni, M. Calligaris, W.M. Attia, Synthesis and characterization of two new classes of ruthenium(III)-sulfoxide complexes with nitrogen donor ligands (L): Na[trans-$RuCl_4(R_2SO)(L)$] and mer, cis-$RuCl_3(R_2SO)(R_2SO)(L)$. The crystal structure of Na[trans-$RuCl_4(DMSO)(NH_3)$] · 2DMSO, Na[trans-$RuCl_4(DMSO)(Im)$] · H_2O, Me_2CO (Im = imidazole) and mer, cis-$RuCl_3(DMSO)(DMSO)(NH_3)$, Inorg. Chim. Acta 203 (1993) 205–217.

[65] A.H. Velders, A. Bergamo, E. Alessio, E. Zangrando, J.G. Haasnoot, C. Casarsa, M. Cocchietto, S. Zorzet, G. Sava, Synthesis and Chemical–Pharmacological Characterization of the Antimetastatic NAMI-A-Type Ru(III) Complexes (Hdmtp)[trans-$RuCl_4$(dmso-S)(dmtp)], (Na)[trans-$RuCl_4$(dmso-S)(dmtp)], and [mer-$RuCl_3(H_2O)$(dmso-S)(dmtp)] (dmtp = 5,7-Dimethyl[1,2,4]triazolo [1,5-a]pyrimidine), J. Med. Chem. 47 (2004) 1110–1121.

[66] M. Delferro, L. Marchiò, M. Tegoni, S. Tardito, R. Franchi-Gazzola, M. Lanfranchi, Synthesis, structural characterisation and solution chemistry of ruthenium(III) triazole-thiadiazine complexes, Dalton Trans. (2009) 3766–3773.

[67] M. Groessl, E. Reisner, C.G. Hartinger, R. Eichinger, O. Semenova, A.R. Timerbaev, M.A. Jakupec, V.B. Arion, B.K. Keppler, Structure–Activity relationships for NAMI-A-type complexes (HL)[trans-$RuCl_4L$(S-dmso)ruthenate(III)] (L = imidazole, indazole, 1,2,4-triazole, 4-Amino-1,2,4-triazole, and 1-Methyl-1,2,4-triazole): aquation, redox properties, protein binding, and antiproliferative activity, J. Med. Chem. 50 (2007) 2185–2193.

[68] I. Turel, M. Pečanac, A. Golobič, E. Alessio, B. Serli, A. Bergamo, G. Sava, Solution, solid state and biological characterization of ruthenium(III)-DMSO complexes with purine base derivatives, J. Inorg. Biochem. 98 (2004) 393–401.

[69] V. Vichai, K. Kirtikara, Sulforhodamine B colorimetric assay for cytotoxicity screening, Nat. Protoc. 1 (2006) 1112–1116.

[70] É. Caron-Beaudoin, J.T. Sanderson, M.S. Denison, Effects of neonicotinoids on promoter-specific expression and activity of aromatase (CYP19) in human adrenocortical carcinoma (H295R) and primary umbilical vein endothelial (HUVEC) cells, Toxicol. Sci. 149 (2015) 134–144.

[71] J.T. Sanderson, W. Seinen, J.P. Giesy, M. van den Berg, 2-Chloro-s-Triazine herbicides induce aromatase (CYP19) activity in H295R human adrenocortical carcinoma cells: a novel mechanism for estrogenicity? Toxicol. Sci. 54 (2000) 121–127.

[72] M. Di Nunzio, V. Valli, L. Tomás-Cobos, T. Tomás-Chisbert, L. Murgui-Bosch, F. Danesi, A. Bordoni, Is cytotoxicity a determinant of the different in vitro and in vivo effects of bioactives? BMC Complement Altern. Med. 17 (2017), 453-453.

[73] M.J. Garle, J.H. Fentem, J.R. Fry, In vitro cytotoxicity tests for the prediction of acute toxicity in vivo, Toxicol. In Vitro 8 (1994) 1303–1312.

[74] F. Joris, B.B. Manshian, K. Peynshaert, S.C. De Smedt, K. Braeckmans, S.J. Soenen, Assessing nanoparticle toxicity in cell-based assays: influence of cell culture parameters and optimized models for bridging the in vitro–in vivo gap, Chem. Soc. Rev. 42 (2013) 8339–8359.

[75] M. Ni, Y. Chen, E. Lim, H. Wimberly, Shannon T. Bailey, Y. Imai, David L. Rimm, X. Shirley Liu, M. Brown, Targeting androgen receptor in estrogen receptor-negative breast cancer, Cancer Cell 20 (2011) 119–131.

[76] A. Valente, M.H. Garcia, F. Marques, Y. Miao, C. Rousseau, P. Zinck, First polymer "ruthenium-cyclopentadienyl" complex as potential anticancer agent, J. Inorg. Biochem. 127 (2013) 79–81.

[77] L. Côrte-Real, A.P. Matos, I. Alho, T.S. Morais, A.I. Tomaz, M.H. Garcia, I. Santos, M.P. Bicho, F. Marques, Cellular uptake mechanisms of an antitumor ruthenium compound: the endosomal/lysosomal system as a target for anticancer metal-based drugs, Microsc. Microanal. 19 (2013) 1122–1130.

[78] L. Côrte-Real, B. Karas, A.R. Brás, A. Pilon, F. Avecilla, F. Marques, A. Preto, B.T. Buckley, K.R. Cooper, C. Doherty, M.H. Garcia, A. Valente, Ruthenium–cyclopentadienyl bipyridine–biotin based compounds: synthesis and biological effect, Inorg. Chem. 58 (2019) 9135–9149.

[79] C. Scolaro, A. Bergamo, L. Brescacin, R. Delfino, M. Cocchietto, G. Laurenczy, T.J. Geldbach, G. Sava, P.J. Dyson, In vitro and in vivo evaluation of ruthenium(II)–Arene PTA complexes, J. Med. Chem. 48 (2005) 4161–4171.

[80] A.K. Renfrew, A.D. Phillips, A.E. Egger, C.G. Hartinger, S.S. Bosquain, A.A. Nazarov, B.K. Keppler, L. Gonsalvi, M. Peruzzini, P.J. Dyson, Influence of structural variation on the anticancer activity of RAPTA-type complexes: ptn versus pta, Organometallics 28 (2009) 1165–1172.

[81] S. Maurelli, M. Chiesa, E. Giamello, G. Di Nardo, V.E.V. Ferrero, G. Gilardi, S. Van Doorslaer, Direct spectroscopic evidence for binding of anastrozole to the iron heme of human aromatase. Peering into the mechanism of aromatase inhibition, Chem. Commun. (J. Chem. Soc. Sect. D) 47 (2011) 10737–10739.

[82] J. Zhao, D. Zhang, W. Hua, W. Li, G. Xu, S. Gou, Anticancer activity of bifunctional organometallic Ru(II) arene complexes containing a 7-hydroxycoumarin group, Organometallics 37 (2018) 441–447.

[83] Y. Liu, N.J. Agrawal, R. Radhakrishnan, A flexible-protein molecular docking study of the binding of ruthenium complex compounds to PIM1, GSK-3β, and CDK2/Cyclin A protein kinases, J. Mol. Model. 19 (2013) 371–382.

[84] P. Mandal, B.K. Kundu, K. Vyas, V. Sabu, A. Helen, S.S. Dhankhar, C.M. Nagaraja, D. Bhattacherjee, K.P. Bhabak, S. Mukhopadhyay, Ruthenium(ii) arene NSAID complexes: inhibition of cyclooxygenase and antiproliferative activity against cancer cell lines, Dalton Trans. 47 (2018) 517–527.

[85] J. Weisz, In vitro assays of aromatase and their role in studies of estrogen formation in target tissues, Cancer Res. 42 (1982) 3295–3298.

[86] E.D. Lephart, E.R. Simpson, [45] Assay of aromatase activity, in: Methods in Enzymology, Academic Press, 1991, pp. 477–483.

[87] J.T. Sanderson, J. Boerma, G.W.A. Lansbergen, M. van den Berg, Induction and inhibition of aromatase (CYP19) activity by various classes of pesticides in H295R human adrenocortical carcinoma cells, Toxicol. Appl. Pharm. 182 (2002) 44–54.

[88] O.A. Lenis-Rojas, A.R. Fernandes, C. Roma-Rodrigues, P.V. Baptista, F. Marques, D. Pérez-Fernández, J. Guerra-Varela, L. Sánchez, D. Vázquez-García, M.L. Torres, A. Fernández, J.J. Fernández, Heteroleptic mononuclear compounds of ruthenium(ii): synthesis, structural analyses, in vitro antitumor activity and in vivo toxicity on zebrafish embryos, Dalton Trans. 45 (2016) 19127–19140.

[89] N. Mandrekar, N.L. Thakur, Significance of the zebrafish model in the discovery of bioactive molecules from nature, Biotechnol. Lett. 31 (2008) 171–179.

[90] C.A. MacRae, R.T. Peterson, Zebrafish as tools for drug discovery, Nat. Rev. Drug Discov. 14 (2015) 721–731.

[91] S. Berghmans, P. Butler, P. Goldsmith, G. Waldron, I. Gardner, Z. Golder, F.M. Richards, G. Kimber, A. Roach, W. Alderton, A. Fleming, Zebrafish based assays for the assessment of cardiac, visual and gut function — potential safety screens for early drug discovery, J. Pharmacol. Toxicol. Methods 58 (2008) 59–68.

[92] L. Côrte-Real, B. Karas, P. Gírio, A. Moreno, F. Avecilla, F. Marques, B.T. Buckley, K.R. Cooper, C. Doherty, P. Falson, M.H. Garcia, A. Valente, Unprecedented inhibition of P-gp activity by a novel ruthenium-cyclopentadienyl compound bearing a bipyridine-biotin ligand, Eur. J. Med. Chem. 163 (2019) 853–863.

[93] B.F. Karas, L. Côrte-Real, C.L. Doherty, A. Valente, K.R. Cooper, B.T. Buckley, A novel screening method for transition metal-based anticancer compounds using zebrafish embryo-larval assay and inductively coupled plasma-mass spectrometry analysis, J. Appl. Toxicol. 39 (2019) 1173–1180.

[94] M.O. Albers, E. Singleton, J.E. Yates, F.B. Mccormick, Dinuclear ruthenium(II) carboxylate complexes, in: Inorganic Syntheses, John Wiley and Sons, Inc., 1989.

[95] M. Bruce, N. Windsor, Cyclopentadienyl-ruthenium and -osmium chemistry. IV. Convenient high-yield synthesis of some cyclopentadienyl ruthenium or osmium tertiary phosphine halide complexes, Aust. J. Chem. 30 (1977) 1601–1604.

[96] E. Alessio, G. Balducci, M. Calligaris, G. Costa, W.M. Attia, G. Mestroni, Synthesis, molecular structure, and chemical behavior of hydrogen trans-bis(dimethyl sulfoxide)tetrachlororuthenate(III) and mer-trichlorotris(dimethyl sulfoxide)ruthenium(III): the first fully characterized chloride-dimethyl sulfoxide-ruthenium(III) complexes, Inorg. Chem. 30 (1991) 609–618.

[97] O.V. Dolomanov, L.J. Bourhis, R.J. Gildea, J.A.K. Howard, H. Puschmann, OLEX2: a complete structure solution, refinement and analysis program, J. Appl. Crystallogr. 42 (2009) 339–341.

[98] G. Sheldrick, A short history of SHELX, Acta Crystallogr. A 64 (2008) 112–122.

[99] G. Sheldrick, Crystal structure refinement with SHELXL, Acta Crystallogr. C 71 (2015) 3–8.

[100] C.B. Kimmel, W.W. Ballard, S.R. Kimmel, B. Ullmann, T.F. Schilling, Stages of embryonic development of the zebrafish, Dev. Dynam. 203 (1995) 253–310.

[101] E. Krieger, K. Joo, J. Lee, J. Lee, S. Raman, J. Thompson, M. Tyka, D. Baker, K. Karplus, Improving physical realism, stereochemistry, and side-chain accuracy in homology modeling: four approaches that performed well in CASP8, Proteins: Struct., Funct., Bioinf. 77 (2009) 114–122.

[102] R. Thomsen, M.H. Christensen, MolDock: A new technique for high-accuracy molecular docking, J. Med. Chem. 49 (2006) 3315–3321.